Letter

Transverse-momentum-dependent wave functions of the pion from lattice QCD

Min-Huan Chu,[1,2] Jin-Chen He,[1,3] Jun Hua,[4,5,*] Jian Liang,[4,5] Xiangdong Ji,[3] Andreas Schäfer,[6] Hai-Tao Shu,[6,†] Yushan Su,[3] Ji-Hao Wang,[7,8] Wei Wang,[1,9] Yi-Bo Yang,[7,8,10,11] Jun Zeng,[1] Jian-Hui Zhang,[12,13] and Qi-An Zhang[14]

(Lattice Parton Collaboration)

[1]*INPAC, Shanghai Key Laboratory for Particle Physics and Cosmology, Key Laboratory for Particle Astrophysics and Cosmology (MOE), School of Physics and Astronomy, Shanghai Jiao Tong University, Shanghai 200240, China*
[2]*Yang Yuanqing Scientific Computering Center, Tsung-Dao Lee Institute, Shanghai Jiao Tong University, Shanghai 200240, China*
[3]*Department of Physics, University of Maryland, College Park, Maryland 20742, USA*
[4]*Key Laboratory of Atomic and Subatomic Structure and Quantum Control (MOE), Guangdong Basic Research Center of Excellence for Structure and Fundamental Interactions of Matter, Institute of Quantum Matter, South China Normal University, Guangzhou 510006, China*
[5]*Guangdong-Hong Kong Joint Laboratory of Quantum Matter, Guangdong Provincial Key Laboratory of Nuclear Science, Southern Nuclear Science Computing Center, South China Normal University, Guangzhou 510006, China*
[6]*Institut für Theoretische Physik, Universität Regensburg, D-93040 Regensburg, Germany*
[7]*CAS Key Laboratory of Theoretical Physics, Institute of Theoretical Physics, Chinese Academy of Sciences, Beijing 100190, China*
[8]*School of Fundamental Physics and Mathematical Sciences, Hangzhou Institute for Advanced Study, UCAS, Hangzhou 310024, China*
[9]*Southern Center for Nuclear-Science Theory (SCNT), Institute of Modern Physics, Chinese Academy of Sciences, Huizhou 516000, Guangdong Province, China*
[10]*International Centre for Theoretical Physics Asia-Pacific, Beijing/Hangzhou, China*
[11]*School of Physical Sciences, University of Chinese Academy of Sciences, Beijing 100049, China*
[12]*School of Science and Engineering, The Chinese University of Hong Kong, Shenzhen 518172, China*
[13]*Center of Advanced Quantum Studies, Department of Physics, Beijing Normal University, Beijing 100875, China*
[14]*School of Physics, Beihang University, Beijing 102206, China*

(Received 26 February 2023; revised 22 December 2023; accepted 29 April 2024; published 24 May 2024)

We present a lattice QCD calculation of the transverse-momentum-dependent wave function (TMDWF) of the pion using large-momentum effective theory. Numerical simulations are based on one ensemble with $2+1+1$ flavors of highly improved staggered quarks with lattice spacing $a = 0.121$ fm from the MILC collaboration, and one with $2+1$ flavor clover fermions and tree-level Symanzik gauge action generated by the CLS collaboration with $a = 0.098$ fm. As a key ingredient, the soft function is first obtained by incorporating the one-loop perturbative contributions and a proper normalization. Based on this and the equal-time quasi-TMDWF simulated on the lattice, we extract the TMDWF. The results for both lattice ensembles are compatible and a comparison with a phenomenological parametrization is made. Our studies provide a first attempt of *ab initio* calculation of TMDWFs which will eventually lead to crucial theory inputs for making predictions for exclusive processes under QCD factorization.

DOI: 10.1103/PhysRevD.109.L091503

[*]Corresponding author: junhua@scnu.edu.cn
[†]Corresponding author: hai-tao.shu@ur.de

Introduction. Light-front wave functions (LFWFs) are an important quantity for hadrons in particle physics. They characterize the nonperturbative structure of hadrons, and enter the prediction of a wide variety of measurable observables using quantum chromodynamics (QCD) factorization. While searching for new physics beyond the standard model (SM) requires a dedicated study of high-energy processes at colliders, this goal can partially be achieved by investigating low-energy processes, among which the flavor-changing-neutral-current (FCNC) in a heavy quark system is an ideal probe [1]. A key input for calculating the SM contributions to the FCNC for LFWFs includes the collinear distribution amplitudes (LCDAs) and the transverse-momentum-dependent wave functions (TMDWFs). LFWFs in fact play an essential role in light-front quantization. In particular, the parton distribution functions can be expressed in terms of the square of the TMDWFs [2,3]. The TMDWFs are characterized by physics at transverse distance scale of a Fermi or equivalently momentum scale of a few hundred MeV, which is similar to the confinement scale. Therefore, experimental determinations and theoretical computations of these distributions may help to reveal the nature of nonperturbative phenomena such as confinement and chiral symmetry breaking in QCD.

Although TMDWFs describe important aspects of the three-dimensional structure of hadrons, they have never been studied in the literature from first principles QCD with controlled systematic approximations. Similar to the definition of transverse-momentum-dependent parton distribution functions (TMDPDFs), it is nontrivial to present a rigorous definition of TMDWFs [4]. A key difficulty resides in the rapidity divergences that show up in regularizing the soft contributions from a collinear constituent [5]. So far, most applications of TMD factorization to hard exclusive processes have adopted phenomenological models to parametrize the TMDWFs [6–8], which inevitably introduced uncontrollable systematic uncertainties and compromised precision tests of the SM and probes for new physics.

Large-momentum effective theory (LaMET) [9,10] develops a novel way to extract parton physics from lattice QCD calculations through expansion in large hadron momentum (see [11] for a review and many references therein). For TMDWFs, the calculation requires the knowledge on the so-called soft function, which incorporates the effects of soft gluon radiation from colored collinear particles from two opposite lightlike directions [12,13]. It was recently discovered that the soft function can be determined by calculating a large-momentum-transfer form factor of a light meson and quasi-TMDWFs on the lattice [14,15], which makes it possible to calculate TMDWFs from the lattice QCD [11,16].

In this Letter, we report a first lattice QCD calculation of the pion TMDWF using LaMET. The calculation is performed for two lattice ensembles with three hadron momenta up to 2.63 GeV. We obtain the soft function by incorporating the one-loop perturbative contributions and a proper normalization. Based on this, we present a first result for the physical TMDWF. We get compatible results for both lattice ensembles and a comparison with the phenomenological model is shown.

Theoretical framework. The TMDWF $\Psi^{\pm}(x, b_\perp, \mu, \zeta)$ provides the momentum distribution between the quark and antiquark in the leading pion Fock state. The superscript "$\pm$" denotes that in $\Psi^{\pm}$ Wilson lines will approach the positive and negative infinity along the light cone direction. x denotes the momentum fraction in longitudinal direction, and $b_\perp$ is the Fourier conjugate of transverse momentum. In addition, TMDWFs also depend on the renormalization scale μ and the rapidity scale ζ.

LaMET allows to access the TMDWF $\Psi^{\pm}$ by simulating an equal-time quasi-TMDWF $\tilde{\Psi}^{\pm}$ defined in Euclidean space. The relation between them follows the factorization formula [15,16]:

$$\begin{aligned}
&\tilde{\Psi}^{\pm}(x, b_\perp, \mu, \zeta^z) S_I^{\frac{1}{2}}(b_\perp, \mu) \\
&\quad = H^{\pm}(x, \zeta^z, \mu) e^{[\frac{1}{2}K(b_\perp,\mu)\ln\frac{\mp\zeta^z + i\epsilon}{\zeta}]} \Psi^{\pm}(x, b_\perp, \mu, \zeta) \\
&\qquad + \mathcal{O}\Big(\Lambda_{\rm QCD}^2/(x^2\zeta^z), M^2/(P^z)^2, 1/(b_\perp^2\zeta^z)\Big), \qquad (1)
\end{aligned}$$

where $\zeta^z = (2P^z)^2$. $S_I(b_\perp, \mu)$ denotes the intrinsic soft function. $K(b_\perp, \mu)$ is the Collins-Soper kernel and has been calculated on the lattice in [17–19]. $H^{\pm}(x, \zeta^z, \mu)$ represents a perturbative matching kernel. At one-loop level it is given by [16,20]

$$\begin{aligned}
H^{\pm}(x, \zeta^z, \mu) = 1 + \frac{\alpha_s C_F}{4\pi}\Bigg(&-\frac{5\pi^2}{6} - 4 + l_\pm + \bar{l}_\pm \\
&-\frac{1}{2}(l_\pm^2 + \bar{l}_\pm^2)\Bigg), \qquad (2)
\end{aligned}$$

where $l_\pm = \ln[(-x^2\zeta^z \pm i\epsilon)/\mu^2]$ and $\bar{l}_\pm = \ln[(-\bar{x}^2\zeta^z \pm i\epsilon)/\mu^2]$. x and $\bar{x} = 1 - x$ are the momentum fractions of quark and antiquark. Power corrections in LaMET factorization are generically suppressed by factors $[\Lambda_{\rm QCD}^2/(x^2\zeta^z), M^2/(P^z)^2, 1/(b_\perp^2\zeta^z)]$.

For a Euclidean lattice and a pseudoscalar meson, the equal-time quasi-TMDWF in momentum space $\tilde{\Psi}^{\pm}(x, b_\perp, \mu, \zeta^z)$ can be extracted from a large P^z meson-to-vacuum matrix element of a nonlocal bilinear operator:

$$\begin{aligned}
\tilde{\Psi}^{\pm}(x, b_\perp, \mu, \zeta^z) = \lim_{L\to\infty} \frac{1}{-if_\pi P^z} \int \frac{dzP^z}{2\pi} e^{ixzP^z} \\
\times \frac{\langle 0|\bar{q}(z\hat{n}_z + b_\perp\hat{n}_\perp)\gamma^t\gamma_5 U_{c\pm} q(0)|\pi(P^z)\rangle}{\sqrt{Z_E(2L + |z|, b_\perp, \mu)} Z_O(1/a, \mu)},
\end{aligned} \qquad (3)$$

where we choose $\gamma^t\gamma_5$ to project onto the leading-twist TMDWF, which may suffer from operator mixing effects [21–23]. As an estimate of these effects in the following we include 10% uncertainties to the final results. The staple-shaped Wilson line between the quark fields $U_{c\pm}$ is required:

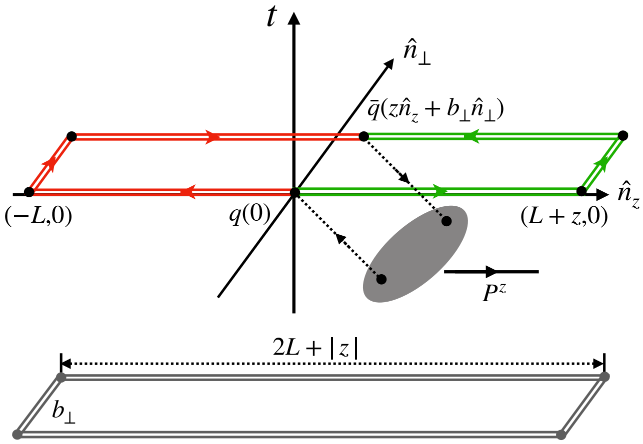

FIG. 1. Illustration of quasi-TMDWF in coordinate space with a staple-shaped Wilson line inside. The green and red double lines represent the Wilson lines in $\tilde{\Psi}^{+}(z, b_\perp, \mu, \zeta^z)$ and $\tilde{\Psi}^{-}(z, b_\perp, \mu, \zeta^z)$. A corresponding staple-shaped Wilson loop $Z_E(2L+|z|, b_\perp, \mu)$ is constructed to cancel the linear and cusp divergences.

$$U_{c\pm} = U_z^\dagger(z\hat{n}_z + b_\perp\hat{n}_\perp; -\bar{L}_\pm)U_\perp(\bar{L}_\pm\hat{n}_z + z\hat{n}_z; b_\perp) \times U_z(0\hat{n}_z; \bar{L}_\pm + z), \tag{4}$$

where $U_\mu(x;l) \equiv U_\mu(x, x+l\hat{n}_\mu)$ and $\bar{L}_\pm \equiv \pm\max(L, L\mp z)$, see Fig. 1. L is the length of path-ordered Euclidean Wilson lines along the z direction. In principle we have to take the $L \to \infty$ limit, but in lattice calculations, we have shown in [18] the $L \simeq 0.7$ fm is sufficient, which is what we use.

The bare matrix element in the numerator in Eq. (3) contains both a pinch pole singularity and a linear divergence which can be removed by the Wilson loop $Z_E(2L+|z|, b_\perp, \mu)$ [15]. The logarithmic divergences arising from the end points of the Wilson line need an additional quark Wilson line vertex renormalization factor $Z_O(1/a, \mu)$. A straightforward way to determine Z_O is to evaluate the quotient of the renormalized quasi-TMDWF calculated on the lattice in the small $b_\perp$ region and the quasi-TMDWF perturbatively calculated in the $\overline{\mathrm{MS}}$ scheme, as discussed in [21]. In practice, we adopt $Z_O = \{0.917(2), 0.903(2)\}$ for MILC and CLS ensembles in this work; for details see the Supplemental Material [24].

Lattice simulation. We use one ensemble of the hypercubic (HYP)-smeared clover valence fermions action on $2+1+1$ flavors of highly improved staggered sea quarks (HISQ) [25] generated by MILC [26] at the lattice spacing $a = 0.121$ fm, and one ensemble of $2+1$ flavor clover fermions generated by the CLS collaboration at $a = 0.098$ fm with the unitary valence fermion action. The rest of the simulation setups are collected in Table I. To improve the signal-to-noise ratio, we adopt hypercubic (HYP) smeared fat links [27] for the staple-shaped gauge link $U_{c\pm}$, and generate the Coulomb gauge fixed wall source propagators S_w to build correlation functions. To access the large-momentum limit, we employ three different hadron momenta $P^z = 2\pi/n_s \times \{4, 5, 6\} = \{1.72, 2.15, 2.58\}$ GeV for the MILC ensemble and $P^z = 2\pi/n_s \times \{6, 8, 10\} = \{1.58, 2.11, 2.64\}$ GeV for the CLS ensemble.

TABLE I. The numerical simulation setup. For each ensemble, we put eight and four source slices in time direction.

Ensemble	a(fm)	$n_s^3 \times n_t$	m_π^{sea} (MeV)	m_π^{val} (MeV)	Measure
a12m310	0.121	$24^3 \times 64$	310	670	1053×8
X650	0.098	$48^3 \times 48$	333	662	911×4

To determine the quasi-TMDWF, one can construct the nonlocal two point correlation function as follows:

$$C_2^\pm(L, z, b_\perp, t, P^z) = \sum_{\vec{x}} e^{iP^z\vec{x}\cdot\hat{n}_z}\langle S_w^\dagger(\vec{x} + z\hat{n}_z + b_\perp\hat{n}_\perp, t)U_{c\pm}S_w(\vec{x}, t)\rangle. \tag{5}$$

Because of the limited L in lattice simulation discussed in Eq. (4), we adopt $(z > 0)$ for C_2^+ and $(z < 0)$ for C_2^-, then the $(z < 0)$ for C_2^+ and $(z > 0)$ for C_2^- can be obtained by isospin symmetry. The symmetry behavior of quasi-TMDWFs for $\pm z$ has been numerically studied in [18].

The ground-state contribution to the quasi-TMDWF can be extracted by the following two-state fit parametrization:

$$\frac{C_2^\pm(L, z, b_\perp, t, P^z)}{C_2^\pm(L, z=0, b_\perp=0, t, P^z)} = \tilde{\Psi}^{\pm,0}(z, b_\perp, \zeta^z, L) \times \frac{1 + c_0(z, b_\perp, P^z, L)e^{-\Delta E t}}{1 + c_1 e^{-\Delta E t}}, \tag{6}$$

where $\tilde{\Psi}^{\pm,0}(z, b_\perp, \zeta^z, L)$ is the bare quasi-TMDWF in coordinate space, while $c_{0,1}$ and ΔE are free parameters accounting for excited state contamination. In the large t limit, this contamination is suppressed exponentially, which gives the possibility to extract the quasi-TMDWF through a one-state parametrization. Comparing one- and two-state fits in the Supplemental Material [24], we find that the one-state fit gives a more stable result which will be used in the following analysis.

Numerical results. After renormalization by Wilson loop Z_E and quark Wilson line vertex correction Z_O in Eq. (3), the quasi-TMDWF in coordinate space can be obtained straightforwardly. As discussed for our hybrid scheme in [28], a brute-force truncation of the Fourier transformation at finite z will introduce unphysical oscillations. To avoid these oscillations, we adopt an analytical

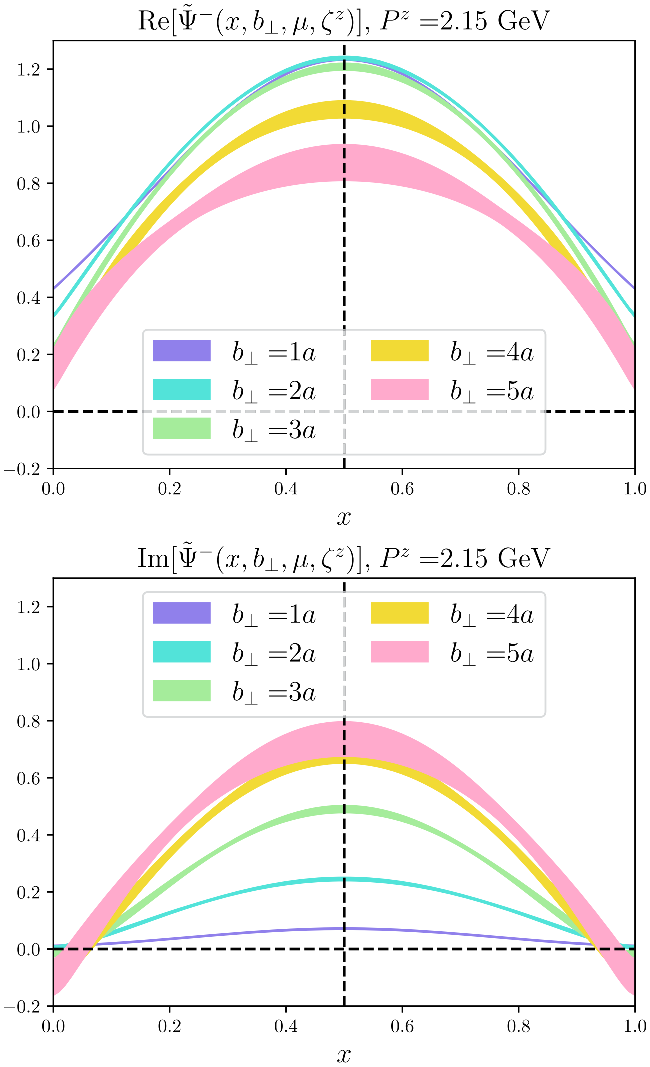

FIG. 2. The real part (upper panel) and the imaginary part (lower panel) of the quasi-TMDWF in momentum space, with hadron momentum $P^z = 2.15$ GeV and for the MILC ensemble.

extrapolation at large light-front distance ($\lambda = zP^z$) for quasi-TMDWFs in coordinate space:

$$\tilde{\Psi}(z, b_\perp, \mu, \zeta^z) = f(b_\perp)\left[\frac{k_1}{(-i\lambda)^d} + e^{i\lambda}\frac{k_2}{(i\lambda)^d}\right]e^{-\frac{\lambda}{\lambda_0}}, \quad (7)$$

where $k_{1,2}, d$ are free parameters, λ_0 denotes a large distance parameter [28,29], and the complex parameter $f(b_\perp)$ describes the behavior in transverse direction. After extrapolation and Fourier transformation, we get the results shown in Fig. 2, for the real part (upper panel) and the imaginary part (lower panel) of the quasi-TMDWF in momentum space at $P^z = 2.15$ GeV for the MILC ensemble. As can be seen from this figure, the real part decreases slowly with increasing $b_\perp$, while the imaginary part increases rapidly with $b_\perp$. Unlike the one dimensional quasi-distribution amplitude in [29], the quasi-TMDWF has a sizable nonzero imaginary part.

According to the LaMET factorization in Eq. (1), apart from the quasi-TMDWF, one requires the intrinsic soft function and Collins-Soper (CS) evolution kernel to obtain the TMDWF. In recent years, the CS kernel has been determined on the lattice [17–19]. A recent analysis for the MILC ensemble at 0.121 fm that includes the one-loop perturbative contributions can be found in Ref. [18], while for the CLS ensemble at 0.098 fm the result is given in the Supplemental Material [24].

The intrinsic soft function can be determined from the quasi-TMDWF and the form factor of a pseudoscalar meson. The calculation of the tree level intrinsic soft function was performed in [30,31]. Inspired by a detailed theoretical analysis of normalization condition and twist combination of the form factor in [20], we present the intrinsic soft function in Fig. 3 that is based on the one-loop matching kernel. As can be seen from this figure, the intrinsic soft functions extracted by $\tilde{\Psi}^{+}$ and $\tilde{\Psi}^{-}$ for the MILC ensemble are consistent with each other, which is in line with the expectation that the intrinsic soft function is universal. The result obtained by $\tilde{\Psi}^{-}$ on the CLS ensemble is similar but the soft function decreases more slowly than the MILC results. A reason for this difference might be discretization effects, which will be further investigated in future work. Our lattice results have similar $b_\perp$ dependence as a one-loop perturbative result in the $\overline{\mathrm{MS}}$ scheme [32] in both the small and large $b_\perp$ regions. However, it is necessary to point out that the perturbative result might be unreliable at large $b_\perp$.

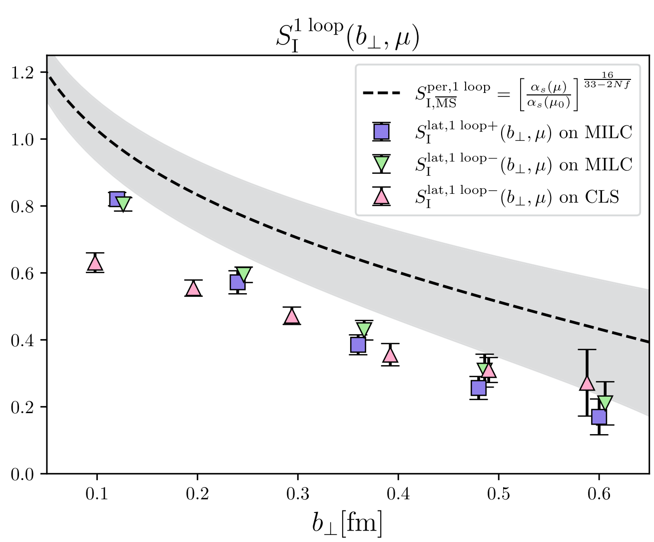

FIG. 3. The one-loop intrinsic soft function as a function of $b_\perp$. The gray band corresponds to the one-loop perturbative result in the $\overline{\mathrm{MS}}$ scheme and the band is obtained by $\mu_0 = 1/b_\perp^*$ varying in the range $b_\perp^* \in [1/\sqrt{2}, \sqrt{2}]b_\perp$. The label $\pm$ in $S^{\mathrm{lat},1\text{ loop}\pm}$ represents the lattice results extracted for $\tilde{\Psi}^{\pm}$.

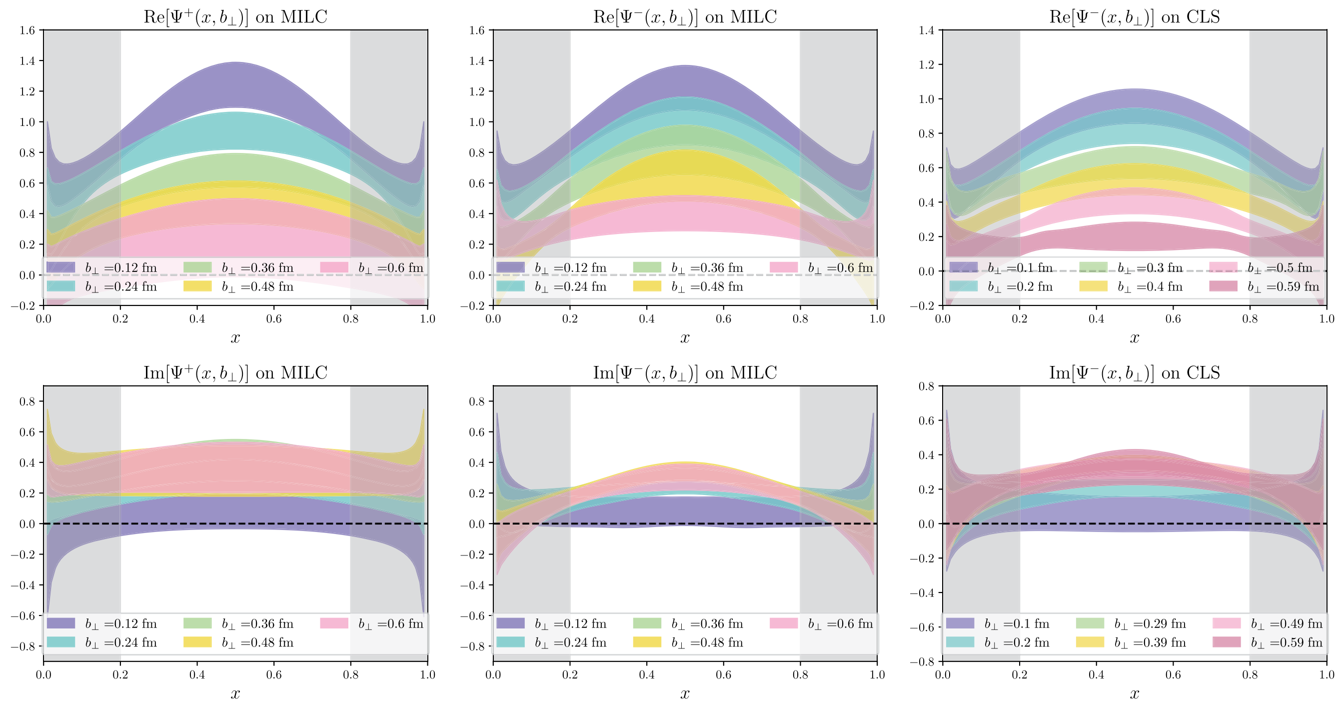

FIG. 4. The left two parts are for real (upper panel) and imaginary parts (lower panel) of the TMDWF Ψ^+, and the central two correspond to Ψ^- all for the MILC ensemble. The right two parts correspond to Ψ^- and the CLS ensemble. These results approach the infinite P^z limit with $\zeta = (6\ \text{GeV})^2$ and $\mu = 2$ GeV.

Together with the quasi-TMDWF, one-loop intrinsic soft function, and CS kernel, the TMDWF can be obtained through a perturbative matching; see Eq. (1). In Fig. 4, we show the final results for TMDWFs $\Psi^\pm$ for the MILC ensemble (left and central panels) and Ψ^- the CLS ensemble (right panel). Results in this figure contain both statistical and systematic uncertainties, where the systematic ones come from the large λ extrapolation and the infinite momentum extrapolation [24]. The renormalization scale is chosen as $\mu = 2$ GeV and the rapidity scale as $\zeta = (2P^+)^2 = (6\ \text{GeV})^2$. As can be seen from the figure, the real part of the TMDWF decreases as $b_\perp$ increases, while the imaginary part first increases and stabilizes for $b_\perp > 0.36$ fm. The imaginary part shows a weaker dependence on $b_\perp$ than the real part, because part of the $b_\perp$ dependence is absorbed into soft function and CS kernel. The Ψ^+ and Ψ^- show a different behavior as $b_\perp$ increases due to the fact that they describe distinct physical properties. Similarly it is known that the Wilson lines in TMD parton distribution functions (TMDPDFs) have opposite directions, which correspond to semi-inclusive deep inelastic scattering and Drell-Yan processes, respectively. Similar properties should be expected for TMDWF in the TMD factorization of the exclusive processes, which however have not been discussed before.

The LaMET factorization [Eq. (1)] will break down in the end point region. Therefore, at present, LaMET results are not under control in the shaded regions ($x < 0.2$ and $x > 0.8$). Furthermore, an estimation for power corrections of $b_\perp$ with $\mathcal{O}(1/(b_\perp^2\zeta^z))$ indicates that our results are more reliable at $b_\perp \geq 0.2$ fm.

In Fig. 5, we show a comparison of TMDWFs $\Psi^\pm$ at the momentum fraction $x = 0.5$ for the MILC and CLS ensembles with a phenomenological model [33], which factorizes TMDWF into longitudinal and transverse

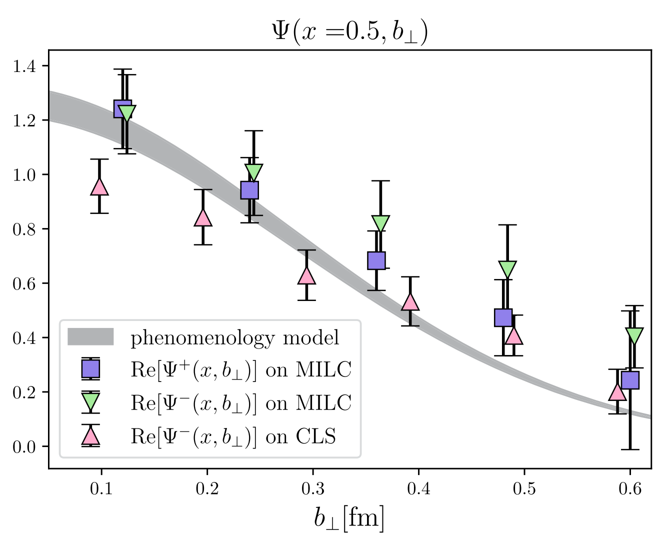

FIG. 5. Comparison of the transverse momentum distribution in our results with $\{\zeta,\mu\} = \{(6\ \text{GeV})^2, 2\ \text{GeV}\}$ and phenomenological model at $x = 0.5$.

momentum distributions. The TMDWFs decay with increasing $b_\perp$, which is consistent with the phenomenological model. However, the phenomenological parametrization only contains the real parts and does not include the difference of Wilson line directions in Eq. (4). These two features show highly relevant complexities that have never been discussed in uses of TMD factorization for the hard exclusive process.

Our numerical results are based on different discretizations and lattice spacings, thus their difference can be considered as an estimate of the discretization error in the absence of further studies at smaller lattice spacings. Besides, our lattice simulations are performed with pion mass around 670 MeV, which is far from the physical point. Therefore, our results are still subject to large systematic uncertainties, and future calculations with smaller lattice spacings and lighter quark masses can significantly improve them.

Summary. We present a first lattice calculation of the transverse-momentum-dependent wave function of the pion. Numerical simulations are conducted for two ensembles by the MILC and CLS collaborations. The linear and logarithmic divergences are canceled by Wilson loop and quark Wilson line vertex correction. The extrapolation strategy for the pion quasi-TMDWF in coordinate space follows the hybrid scheme.

Our final results extracted from both ensembles have a consistent $b_\perp$ dependence, with some differences at small $b_\perp$, which might come from discretization errors. These are the first results of an *ab initio* calculation for a TMDWF which will eventually lead to crucial theory inputs for making predictions for exclusive processes in QCD factorization. The difference between $\Psi^\pm$ and the large imaginary parts of the TMDWF indicates that a more comprehensive TMD factorization for hard exclusive processes is needed.

Acknowledgments. We thank the MIMD Lattice Computation (MILC) Collaboration for providing us their HISQ gauge configurations. We thank the CLS Collaboration for sharing the ensembles used to perform this study. We thank Wolfgang Söldner for valuable discussions on the X650 ensemble. This work is supported in part by Natural Science Foundation of China under Grants No. U2032102, No. 12125503, No. 12205106, No. 12175073, No. 12222503, No. 12293060, No. 12293062, No. 12147140, No. 12205180, No. 12047503, No. 12005130, No. 12335003, No. 12375069. The computations in this paper were run on the Siyuan-1 cluster supported by the Center for High Performance Computing at Shanghai Jiao Tong University, supercomputing system in the Southern Nuclear Science Computing Center, and Advanced Computing East China Sub-center. J. H. and J. L. are also supported by Guangdong Major Project of Basic and Applied Basic Research No. 2020B0301030008. Y. B. Y. is also supported by the Strategic Priority Research Program of Chinese Academy of Sciences, Grants No. XDB34030303 and No. YSBR-101. J. H. Z. is supported in part by National Natural Science Foundation of China under Grant No. 11975051. J. Z. is also supported by the China Postdoctoral Science Foundation under Grant No. 2022M712088. A. S., H. T. S., W. W., Y. B. Y., and J. H. Z. are also supported by a NSFC-DFG joint grant under Grant No. 12061131006 and SCHA~458/22.

[1] G. Buchalla, A. J. Buras, and M. E. Lautenbacher, Rev. Mod. Phys. **68**, 1125 (1996).
[2] S. J. Brodsky, Acta Phys. Pol. B **32**, 4013 (2001), https://www.actaphys.uj.edu.pl/fulltext?series=Reg&vol=32&page=4013.
[3] M. Burkardt, X.-d. Ji, and F. Yuan, Phys. Lett. B **545**, 345 (2002).
[4] J. P. Ma and Q. Wang, Phys. Lett. B **613**, 39 (2005).
[5] J. C. Collins and D. E. Soper, Nucl. Phys. **B194**, 445 (1982).
[6] Y.-Y. Keum, H.-n. Li, and A. I. Sanda, Phys. Lett. B **504**, 6 (2001).
[7] C.-D. Lu, K. Ukai, and M.-Z. Yang, Phys. Rev. D **63**, 074009 (2001).
[8] A. Ali, G. Kramer, Y. Li, C.-D. Lu, Y.-L. Shen, W. Wang, and Y.-M. Wang, Phys. Rev. D **76**, 074018 (2007).
[9] X. Ji, Phys. Rev. Lett. **110**, 262002 (2013).
[10] X. Ji, P. Sun, X. Xiong, and F. Yuan, Phys. Rev. D **91**, 074009 (2015).
[11] X. Ji, Y.-S. Liu, Y. Liu, J.-H. Zhang, and Y. Zhao, Rev. Mod. Phys. **93**, 035005 (2021).
[12] J. C. Collins and D. E. Soper, Nucl. Phys. **B193**, 381 (1981); **B213**, 545(E) (1983).
[13] J. C. Collins, D. E. Soper, and G. F. Sterman, Nucl. Phys. **B308**, 833 (1988).
[14] X. Ji, Y. Liu, and Y.-S. Liu, Phys. Lett. B **811**, 135946 (2020).
[15] X. Ji, Y. Liu, and Y.-S. Liu, Nucl. Phys. **B955**, 115054 (2020).
[16] X. Ji and Y. Liu, Phys. Rev. D **105**, 076014 (2022).
[17] P. Shanahan, M. Wagman, and Y. Zhao, Phys. Rev. D **104**, 114502 (2021).
[18] M.-H. Chu *et al.* (LPC Collaboration), Phys. Rev. D **106**, 034509 (2022).

[19] M. Schlemmer, A. Vladimirov, C. Zimmermann, M. Engelhardt, and A. Schäfer, J. High Energy Phys. 08 (2021) 004.

[20] Z.-F. Deng, W. Wang, and J. Zeng, J. High Energy Phys. 09 (2022) 046.

[21] K. Zhang, X. Ji, Y.-B. Yang, F. Yao, and J.-H. Zhang (Lattice Parton (LPC) Collaboration), Phys. Rev. Lett. **129**, 082002 (2022).

[22] J.-W. Chen, T. Ishikawa, L. Jin, H.-W. Lin, J.-H. Zhang, and Y. Zhao (LP3 Collaboration), Chin. Phys. C **43**, 103101 (2019).

[23] P. Shanahan, M. L. Wagman, and Y. Zhao, Phys. Rev. D **101**, 074505 (2020).

[24] See Supplemental Material at http://link.aps.org/supplemental/10.1103/PhysRevD.109.L091503 for more details of the analysis.

[25] E. Follana, Q. Mason, C. Davies, K. Hornbostel, G. P. Lepage, J. Shigemitsu, H. Trottier, and K. Wong (HPQCD, UKQCD Collaborations), Phys. Rev. D **75**, 054502 (2007).

[26] A. Bazavov *et al.* (MILC Collaboration), Phys. Rev. D **87**, 054505 (2013).

[27] A. Hasenfratz and F. Knechtli, Phys. Rev. D **64**, 034504 (2001).

[28] X. Ji, Y. Liu, A. Schäfer, W. Wang, Y.-B. Yang, J.-H. Zhang, and Y. Zhao, Nucl. Phys. **B964**, 115311 (2021).

[29] J. Hua *et al.* (Lattice Parton Collaboration), Phys. Rev. Lett. **129**, 132001 (2022).

[30] Q.-A. Zhang *et al.* (Lattice Parton Collaboration), Phys. Rev. Lett. **125**, 192001 (2020).

[31] Y. Li *et al.*, Phys. Rev. Lett. **128**, 062002 (2022).

[32] M. A. Ebert, I. W. Stewart, and Y. Zhao, J. High Energy Phys. 09 (2019) 037.

[33] C.-D. Lu, W. Wang, and Y.-M. Wang, Phys. Rev. D **75**, 094020 (2007).